Cascade effects in a nonequilibrium phase transition with metallurgical relevance

P. Bellon and G. Martin*
CECM-CNRS 15 rue Georges Urbain, 94407 Vitry Cedex, France
(Received 14 June 1988)

The order-disorder transition (antiferromagnetic with conserved total spin) is studied when atomic exchanges result from two processes in parallel, as is the case under energetic particle irradiation: thermally activated jumps and ballistic jumps. The latter favor fully disordered configurations (infinite-temperature dynamics), while the former tend to restore some degree of order. The appropriate mean-field phase diagram is established. A tricritical point is identified below which the nonequilibrium order-disorder transition becomes first order. Stochastic effects are addressed by master-equation and Fokker-Planck equation techniques. Introducing ballistic jumps by bursts (replacement cascades) does not change the steady-state values of the order parameter but definitely affects their respective stability. Below the tricritical temperature, cascade effects shift the phase boundary of the first-order transition towards the spinodal ordering line.

I. INTRODUCTION

Nonequilibrium phase transitions, i.e., transitions between steady states of a dynamical system, rather than between equilibrium states of a thermodynamical system, are of interest in a large variety of fields:[1] physical chemistry,[2] electrical engineering,[3] and materials science.[4] One example of such nonequilibrium phase transitions in condensed-matter physics is given by irradiation-induced phase transitions.[5] The latter occur when atoms are ejected from their equilibrium position by nuclear collisions. The configuration of the system results, in most simple examples, from a competition between irradiation-induced disorder due to atomic jumps induced by nuclear collisions (ballistic jumps) and thermally activated reordering due to the usual atomic jumps (thermal jumps of point defects). One may say that the configuration space of such systems is explored following two dynamics which act in parallel: the usual thermal jumps, which favor the occupancy of low-energy configurations, and the ballistic jumps which occur irrespective of the value of the energy of the configuration. Under the effect of ballistic jumps only, the configuration space is explored as it would be at infinite temperature. In a previous work,[6] we showed that, with some simplifying assumptions, in the particular case of the unmixing transition (ferromagnetic transition with conserved total spin), the steady-state configuration of the system under irradiation at temperature T is the thermodynamical equilibrium configuration of the same system at a higher temperature $T'=(1+\gamma)T$, where γ is the ratio of the ballistic to thermal atom jump frequency (respectively, Γ_b and Γ_t).

Here we examine the order-disorder transition for the $B2$ (β-brass) structure, an interesting one because of its simplicity and relevance to metallurgy. From a very simple mean-field description of the thermodynamics and of the kinetics of this phase transition we build the appropriate phase diagram: the temperature–ballistic jump frequency plane is shared into two fields, that of the ordered and that of the disordered phase. We show that the phase transition which is of second order in the purely thermodynamical case becomes first order at low enough a temperature. The temperature at which this change occurs (tricritical point) is predicted to be $T_c/(1+\gamma^*)$, where T_c is the critical temperature and $\gamma^*=(1+\sqrt{3})/2$. Moreover, using a master-equation technique, we show how the above phase diagram is affected by "cascade effects:" indeed, under practical conditions, ballistic jumps rarely occur individually; usually a stack of atoms is shifted at once, along so-called replacement collisions sequences,[7(a)] or inside "displacement cascades."[7(b)] Depending on the details of the nuclear collision process, 10 to more than 100 atoms may exchange position at once. We show that cascade effects do not change the steady-state values of the order parameter, which are correctly predicted by the deterministic kinetic model, but significantly modify the respective stability of the various steady states. Indeed, the first-order transition line is shifted towards the spinodal ordering line when the cascade size increases.

Let us quote that some of the effects we have identified are reminiscent of what has been observed in the kinetic Ising model with several competing dynamics, either in numerical experiments or in an analytical way.[8] However, cascade size effects have not yet been studied to our knowledge.

The paper proceeds as follows. We first recall the classical mean-field treatment of the thermodynamics,[9] and the rate theory of the kinetics[10] of the order-disorder transition in the $B2$ structure. In Sec. III we introduce ballistic effects in the above rate theory and point to the occurrence of a tricritical point in the dynamical phase diagram. The latter is discussed in detail in Sec. IV. A stochastic description of the transition is introduced in Sec. V; we build a master equation, the steady-state solution of which coincides, in the absence of external forcing, with that of the thermodynamical model: both models yield the same probability distribution for the macrostates. When the ballistic jumps are operating, a stochas-

tic potential which do not reduce to the free energy is found. In Sec. VI a Fokker-Planck approximation of the latter master equation is introduced to handle cascade effects. The resulting phase diagram is discussed in Sec. VII.

II. ORDER-DISORDER TRANSITION OUTSIDE IRRADIATION: STATICS AND KINETICS

We consider A and B atoms in 2Ω sites in a bcc lattice; Ω belong to sublattice α, Ω to sublattice β. We call C_α (C_β) the B atomic fraction on sublattice α (β) and ω the ordering energy $[2\omega=8(\varepsilon_{AA}+\varepsilon_{BB}-2\varepsilon_{AB})]$, where ε_{ij} is the contribution of an ij pair of atoms to the internal energy. For the sake of simplicity, we restrict to the stoechiometric composition (which implies $C_\alpha+C_\beta=1$) and to nearest-neighbor interactions. We introduce the long-range order parameter $S=2C_\alpha-1$ and restrict ourselves to the case $0.5\leq C_\alpha\leq 1$; $S=1$ for the fully ordered case $C_\alpha=1$, and $S=0$ for the fully disordered case $C_\alpha=\frac{1}{2}$. In the following, we drop the index α. Simple bound counting gives the free-energy function per atomic site,

$$f(C)=2\omega C(1-C)+k_BT[C\ln C+(1-C)\ln(1-C)] . \tag{1}$$

At equilibrium ($\partial f/\partial C=0$)

$$\frac{C}{1-C}=\exp[2\beta\omega(2C-1)] , \tag{2}$$

where $\beta=(k_BT)^{-1}$. From Eq. (2), the values of S which make $f(C)$ an extremum are solution of the implicit equation[9]

$$S=\tanh(ST_c/T) , \tag{3}$$

with the critical temperature $T_c=\omega/k_B$. Depending on T_c/T, Eq. (3) exhibits one or two solutions (Fig. 1). The transition thus described is of second order.

Equations (2) and (3) may also be considered as yielding the steady-state solution of the following model for the kinetics of the order-disorder transition outside irradiation: since in the $B2$ structure all eight nearest neighbors of an α site are on the β sublattice and vice versa, the time evolution of C_α, which describes the kinetics of the transition, is written as[10]

$$\frac{dC_\alpha}{dt}=-8\Gamma_{\alpha\beta}C_\alpha(1-C_\beta)+8\Gamma_{\beta\alpha}C_\beta(1-C_\alpha) , \tag{4}$$

where Γ_{ij} is the exchange frequency of one B atom from sublattice i to sublattice j and $C_i(1-C_j)$ the probability that one such exchange extracts one B atom from lattice i and replaces it by one A atom from lattice j. The steady-state solution $\bar{C}$ of Eq. (4), with the notations of Eqs. (1)–(4), is written as

$$\left[\frac{\bar{C}}{1-\bar{C}}\right]^2=\Gamma_{\beta\alpha}/\Gamma_{\alpha\beta} , \tag{5}$$

which reduces to Eq. (2) if we set

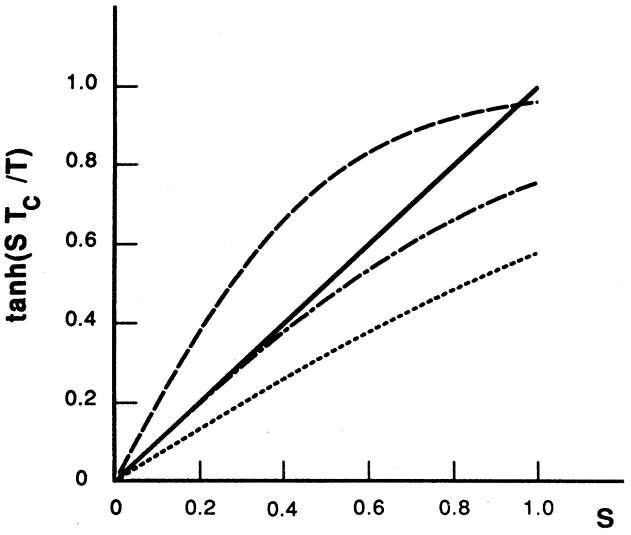

FIG. 1. Construction of the steady-state degrees of order outside irradiation: the solutions of Eq. (3) are at the intersections of the first bisector (——) with $\tanh(ST_c/T)$. The transition is a second-order one: $T/T_c=1.5$ (---); $T/T_c=1.0$ (—·—); $T/T_c=0.5$ (— — —).

$$\Gamma_{\alpha\beta}/\Gamma_{\beta\alpha}=\exp(-4ST_c/T) . \tag{6}$$

The steady-state solution of the kinetic model is thus identical to the equilibrium solution of the thermodynamical model and is obtained by the graphical construction of Fig. 1.

III. BALLISTIC EFFECTS

When ballistic jumps occur in parallel with the thermally activated jumps, the jump frequencies which enter Eq. (4) become

$$\Gamma'_{ij}=\Gamma_{ij}+\Gamma_b , \tag{7}$$

where Γ_b is the ballistic jump frequency which does not depend on the alloy configuration. Let us introduce an average thermal jump frequency Γ_t, such that [following Eq. (6)]

$$\Gamma_{\alpha\beta}=\Gamma_t\exp(-2ST_c/T),\quad \Gamma_{\beta\alpha}=\Gamma_t\exp(2ST_c/T) . \tag{8}$$

Γ_t is a thermally activated average jump frequency, independent of the configuration of the system. Since Γ_t is proportional to the average point defect concentration, it is a function of the temperature and irradiation flux.[6] We define $\gamma=\Gamma_b/\Gamma_t$. The steady-state value of the order parameter under irradiation $\bar{S}'$ is given now as the solution of the implicit equation

$$\left[\frac{1+S}{1-S}\right]^2=\frac{\exp(2ST_c/T)+\gamma}{\exp(-2ST_c/T)+\gamma} \tag{9}$$

or

$$S=U(S) , \tag{10a}$$

with

$$U(S) = \frac{[\gamma+\exp(2ST_c/T)]^{1/2}-[\gamma+\exp(-2ST_c/T)]^{1/2}}{[\gamma+\exp(2ST_c/T)]^{1/2}+[\gamma+\exp(-2ST_c/T)]^{1/2}} . \quad (10b)$$

$\bar{S}'$ is obtained by a graphical construction similar to that of Fig. 1, but $\tanh(ST_c/T)$ is now replaced by $U(S)$ as defined in Eq. (10b). Simple but lengthy algebra shows the following (Fig. 2): introducing $\gamma^*=(1+\sqrt{3})/2$, we find that (a) for $\gamma<\gamma^*$, $U(S)$ exhibits a single inflexion point at the origin. The order-disorder transition is of second order as before; the critical temperature is $T_c/(1+\gamma)$ [see Fig. 2(a)]. (b) For $\gamma\geq\gamma^*$, $U(S)$ exhibits a second inflexion point. (c) At $T^*=T_c/(1+\gamma^*)$, the second inflexion point merges with the first one at the origin. Below this temperature, provided γ is large enough, $U(S)$ cuts the bisector S at three points, one of which is an unstable solution, indicating the transition is of first order [see Fig. 2(b)]. Indeed, a Lyapunov function $\mathcal{L}(S)$ for Eq. (4) is simply

$$\mathcal{L}(S)=-8\int_0^S[\Gamma_{\beta\alpha}(1-C)^2-\Gamma_{\alpha\beta}C^2]d\sigma , \quad (11)$$

where C and Γ_{ij} are functions of the current value σ of the order parameter. When ballistic jumps are operating, Γ_{ij} are to be replaced by Γ'_{ij} as given by Eq. (7). $\mathcal{L}(S)$ exhibits the shapes depicted in Fig. 3, which are reminis-

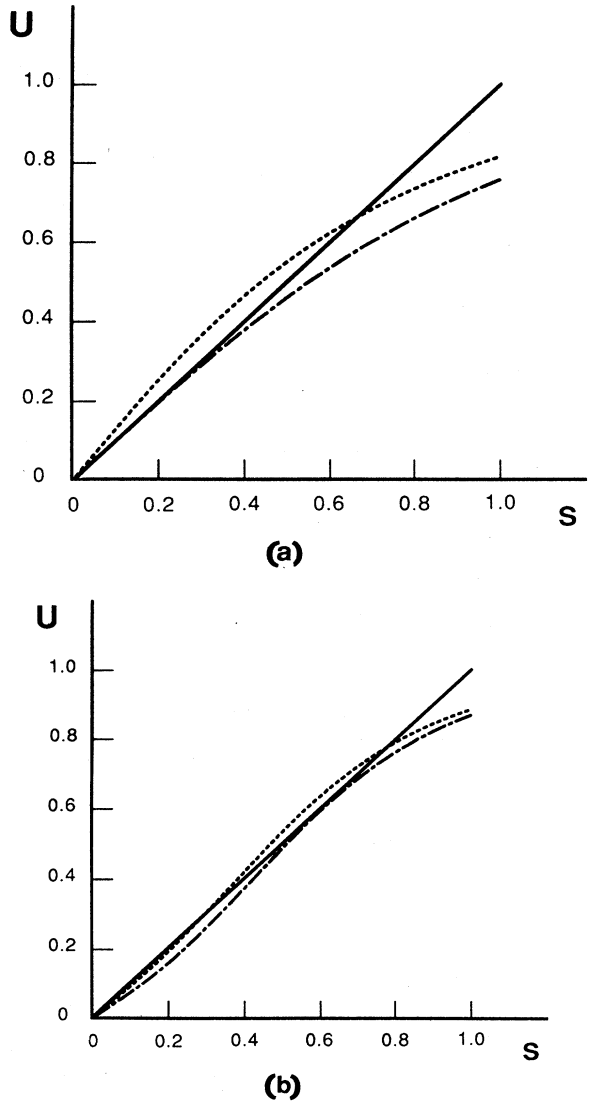

FIG. 2. Construction of the steady-state degrees of order under irradiation: the solutions of Eq. (10) correspond to the intersections of the first bisector (——) with $U(S)$ (which is dimensionless). (a) $T=500\ K>T^*$ and $\gamma<\gamma^*$: $\gamma=0.53$ (---) or $\gamma=1.00$ (—·—); the transition is a second-order one. (b) $T=300$ K $<T^*$ and $\gamma>\gamma^*$: $\gamma=2.84$ (---) or $\gamma=3.79$ (—·—), the transition is a first-order one.

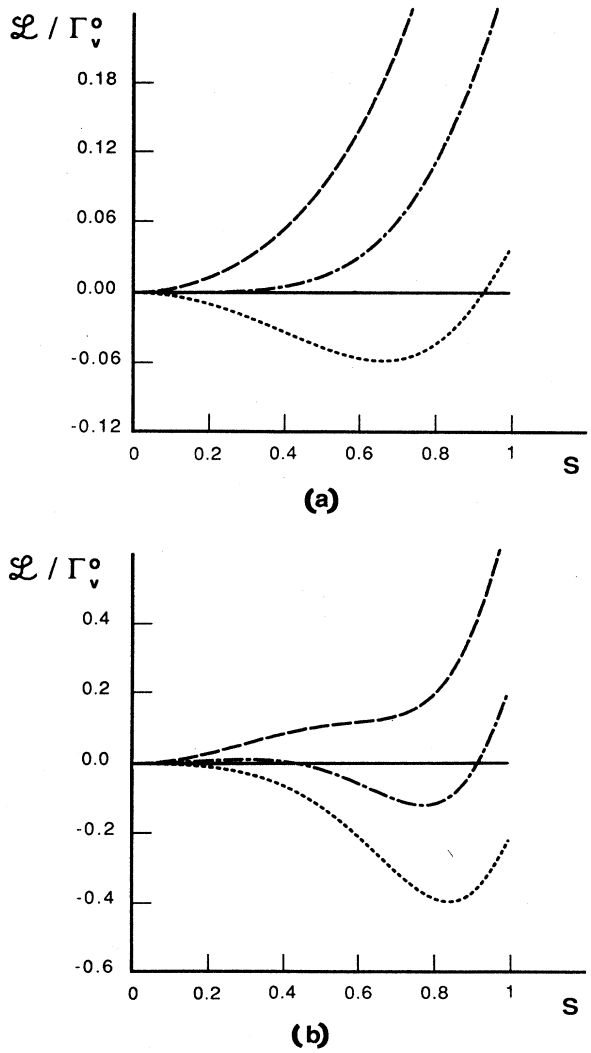

FIG. 3. Lyapunov functions in the presence of ballistic jumps. (a) $T=500$ K and $\gamma=0.53$ (---), $\gamma=1.00$ (—·—), and $\gamma=1.59$ (— — —); (b) $T=300$ K and $\gamma=2.01$ (---), $\gamma=2.84$ (—·—), and $\gamma=3.79$ (— — —). Steady states correspond to extrema of $\mathcal{L}$; the stable one are local minima of $\mathcal{L}$ [Eq. (11)]. $\mathcal{L}$ is given in $(\Gamma_v^0)^{-1}$ units [Eq. (12b)].

cent of the shapes of a mean-field free-energy function for, respectively, second-[case (a)] and first- [case (b)] order phase transitions.

IV. PHASE DIAGRAM

The steady-state configuration of the dynamical system is dictated by two control parameters: the temperature T and the ballistic jump frequency Γ_b which is scaled by the irradiation flux. The dimensionless parameter γ in Eq. (9) is indeed a function of Γ_b and T. The temperature dependence of γ is worth further attention, since Γ_t under irradiation is proportional to the mean point defect concentration which is itself a function of the irradiation flux and temperature. Assuming that a steady-state point defect concentration is obtained by Frenkel pair mutual recombination, we get[6]

$$\gamma = g(b\Gamma_b)^{1/2}(\Gamma_v)^{-1/2} \tag{12a}$$

with g a geometrical factor, $2b$ the number of replaced atoms per cascade, and Γ_v the mean vacancy jump frequency

$$\Gamma_v = \Gamma_v^0 \exp(-\beta E_v^m) \ . \tag{12b}$$

In Eq. (12b), E_v^m is the vacancy migration energy. In the following, for numerical applications, E_v^m is set equal to 1 eV, a typical value in metallurgy. Combining Eqs. (12a) and (12b) we get

$$\gamma = \gamma_0 \exp(\beta E_v^m/2) \ , \tag{12c}$$

where $\gamma_0 = g(b\Gamma_b/\Gamma_v^0)^{1/2}$. In the following, we will define irradiation conditions by γ_0 and T. The phase diagrams will be drawn in the $\gamma_0 - T$ plane. The latter form, although nonuniversal, is more convenient for the experimentalists who adjust independently the irradiation flux (scaled by Γ_b) and the temperature T.

For each value of the couple (γ_0, T) Eqs. (10) may be solved, e.g., by graphical means (Fig. 2). Depending on (γ_0, T), we get one solution ($S=0$) or two solutions ($S=0$, $S=\bar{S}'$) or three solutions (one unstable S_u, two locally stable: $S=0$ and $S=\bar{S}'$). The boundary between one and two solutions is the (second-order) transition line in the (γ_0, T) phase diagram (Fig. 4). The line along which the unstable solution S_u is degenerated as $\bar{S}=0$ is the spinodal ordering line. The latter merges with the former transition line at a tricritical point located at γ^* and T^*, such that $T^* = T_c/a$, $\Gamma_b^* = (a-1)\Gamma_t(T^*)$, and $a = (3+\sqrt{3})/2$. Beyond this point, the transition is of second order, as the thermal phase transition ($\Gamma_b = 0$). When three solutions exist, we are in the vicinity of a first-order transition line. The latter occurs when the respective stability of the two locally stable solutions is reversed. The precise localization of the first-order transition line requires evaluating the respective stability of the solutions. This will be done in Sec. V. Below the tricritical temperature T^*, the transition line in Fig. 4 was drawn from the data of Sec. V. In that region, the transition should exhibit metastability in the region between the transition and the spinodal lines. In this region, the radiation-induced transition should proceed by domain growth. Notice that the tricritical point is defined in a universal way $[\gamma^* = (1+\sqrt{3})/2, \ T^*/T_c = 2/(3+\sqrt{3})]$. However, the $\gamma_0 - T/T_c$ phase diagram is material dependent, since, from Eqs. (12), $\gamma_0^* = \gamma^* \exp(-E_v^m/2kT^*)$. In Fig. 4 and in the following we chose $T_c = 1000$ K, which yield $\gamma_0^* = 1.55 \times 10^{-6}$. With typical material values for γ in Eq. (12a), the displacement rate at the tricritical point would be of the order of 10^{-3} displacement per atom per second, a value typical of high-voltage electron microscopy or of heavy-ion implantation.

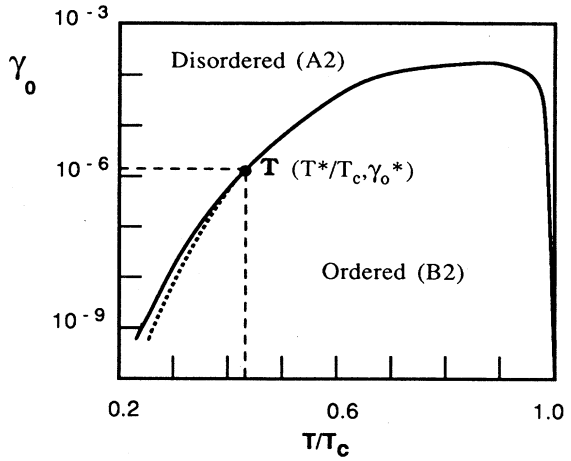

FIG. 4. Dynamical phase diagram. The transition is of second order beyond the tricritical temperature $T^*/T_c = 2/(3+\sqrt{3})$ and first order below $T^* T_c$; the dashed line corresponds to the spinodal ordering line. γ_0 is dimensionless [Eq. (12a)].

V. CASCADE EFFECTS: MASTER-EQUATION DESCRIPTION

We now address the question of cascades, which is of prime interest in metallurgy. We want to check whether the phase diagram just constructed is changed when several ballistic jumps occur simultaneously, keeping γ_0 a constant. In most metallurgical processes (irradiation effects, shear-induced precipitate dissolution), disorder is introduced by shifting $2b$ atoms at once; the frequency at which such "replacement cascades" occur, per α site, is

$$\Gamma_c = \Gamma_b/b \ . \tag{13}$$

For addressing such a question, we need a stochastic description of the kinetics of the transition. This is achieved using a master-equation technique.[11] We define the state of the system by the number N_α of α sites occupied by B atoms. Let $P(N_\alpha, t)$ be the probability of the value N_α at time t for given initial conditions. The time evolution of P is governed by

$$\frac{dP(N_\alpha,t)}{dt} = \sum_{k=1}^{b} [-P(N,t)(W_{N\to N-k} + W_{N\to N+k}) + P(N-k,t)W_{N-k\to N} + P(N+k,t)W_{N+k\to N}] \ . \tag{14}$$

On the right-hand side of Eq. (14), we dropped the α subscript. Equation (14) implies that whenever $2b$ atoms jump at once, exchanges occur among b sites of both sublattices. In Eq. (14), $W_{N\to N+k}$ is the probability that the number of B atoms on sublattice α increases from N to $N+k$ per unit time. Such probabilities may be constructed from the atomistic jump frequencies $\Gamma_{\alpha\beta}$ and $\Gamma_{\beta\alpha}$ and the cascade frequency Γ_c. In the purely thermal case ($\Gamma_c=0$), k values are restricted to 1, and the W's are written as

$$W^t_{N\to N+1}=8\Omega\left[\frac{\Omega-N}{\Omega}\right]^2\Gamma_{\beta\alpha}\left[\frac{N}{\Omega}\right], \tag{15a}$$

$$W^t_{N\to N-1}=8\Omega\left[\frac{N}{\Omega}\right]^2\Gamma_{\alpha\beta}\left[\frac{N}{\Omega}\right], \tag{15b}$$

$$W^t_{N+1\to N}=8\Omega\left[\frac{N+1}{\Omega}\right]^2\Gamma_{\alpha\beta}\left[\frac{N+1}{\Omega}\right], \tag{15c}$$

$$W^t_{N-1\to N}=8\Omega\left[\frac{\Omega-N+1}{\Omega}\right]^2\Gamma_{\beta\alpha}\left[\frac{N-1}{\Omega}\right]. \tag{15d}$$

In Eqs. (15), Γ_{ij} is a function of N/Ω (i.e., of C or of S), as defined by Eq. (8). The superscript (t) implies we are dealing with thermal jumps. When replacement cascades are operating, a ballistic contribution W^b must be added to the thermal transition probabilities. Assuming a replacement cascade consists in $2b$ atoms exchanging position at once with their nearest neighbor, $W^b_{N\to N\pm k}$ is written as

$$W^b_{N\to N\pm k}=8\Omega\Gamma_c\left[\frac{N}{\Omega}\right]^{b\mp k}\left[\frac{\Omega-N}{\Omega}\right]^{b\pm k}\times\frac{(2b)!}{(b-k)!(b+k)!}. \tag{16}$$

$W^b_{N\pm k\to N}$ are deduced straightforwardly from Eq. (16). We are interested in the steady-state solution of Eq. (14). The latter is a conservation equation for the probability at each "site" of the N axis, so that the rhs of Eq. (14) may be considered as the difference between the net flux of probability between sites $N-1$ and N on the one hand, and N and $N+1$ on the other hand. Since systems with $N=0$ or Ω can be neither created nor destroyed, each of the above flux must be zero under steady-state conditions. We get

$$\sum_{m=1}^{b}\sum_{k=m}^{b}P_{N+1-m}W_{N+1-m\to N+1+k-m}=\sum_{m=1}^{b}\sum_{k=m}^{b}P_{N+m}W_{N+m\to N+m-k}. \tag{17}$$

In the particular case where $b=1$, we get the usual form of detailed balance,

$$P_N W_{N\to N+1}=P_{N+1}W_{N+1\to N}. \tag{18}$$

Time does not appear in Eq. (18), since we deal with steady states. We now consider the purely thermal case ($\Gamma_c=0$) and the case of simple ballistic jumps: $\Gamma_c\neq 0$, $b=1$.

A. Purely thermal case

Equation (18) together with the definition of W by Eqs. (15) yield for the steady state

$$\frac{P_{N+1}}{P_N}=\frac{W_{N\to N+1}}{W_{N+1\to N}}=\left[\frac{\Omega-N}{N+1}\right]^2\frac{\Gamma_{\beta\alpha}(N/\Omega)}{\Gamma_{\alpha\beta}[(N+1)/\Omega]}. \tag{19a}$$

Simple iterative use of Eq. (19) yields

$$\frac{P(N)}{P(\Omega/2)}=\prod_{i=\Omega/2}^{N}\left[\left[\frac{\Omega-i-1}{i}\right]^2\times\exp\left[+4\frac{(2i-1-\Omega)T_c}{\Omega T}\right]\right] \tag{20a}$$

$$=\exp\left[\sum_{i=\Omega/2}^{N}\left[+4\frac{(2i-1-\Omega)T_c}{\Omega T}\right]+2\ln\prod_{i=\Omega/2}^{N}\frac{\Omega-i-1}{i}\right]. \tag{20b}$$

As we are interested in calculating these probabilities in the thermodynamical limit, i.e., when $\Omega\to\infty$, N/Ω fixed, we perform a Ω^{-1} expansion of the rhs of Eq. (20b). Retaining the first term of this expansion and taking advantage of Stirling's formula to expand the log term, we get

$$\frac{P(N)}{P(\Omega/2)}=\exp\{-2\Omega[f(C)-f(\tfrac{1}{2})]/kT\}, \tag{21}$$

where $f(C)$ is the free-energy function defined by Eq. (1). Under steady-state conditions, the most probable configuration [$P(N)$ max] corresponds to the absolute minimum of $f(C)$. In other words the kinetic model just considered yields the same probability distribution of configurations as the mean-field thermodynamical model of Sec. II. We can therefore rely on the kinetic model to address nonequilibrium situations.

B. Simple ballistic case: $b=1$

When both thermal jumps and single ballistic jumps are operating, Eq. (18) still holds for the detailed balance, with

$$W_{i\to j}=W^t_{i\to j}+W^b_{i\to j}. \tag{22}$$

From Eqs. (16) and (19), we get

$$\frac{P_{N+1}}{P_N}=\left[\frac{\Omega-N}{N+1}\right]^2\frac{\Gamma_{\beta\alpha}(N/\Omega)+\Gamma_c}{\Gamma_{\alpha\beta}[(N+1)/\Omega]+\Gamma_c}. \tag{23}$$

We can still obtain $P(N)/P(\Omega/2)$ in a form similar to Eq. (20b), but, the $\sum$ term in the argument of the exponential will be much more complicated. Following a standard notation,[2] we get

$$\frac{P(N)}{P(\Omega/2)}=\exp\{2\Omega[\psi(S)-\psi(\tfrac{1}{2})]\}, \tag{24}$$

where ψ (as did the free energy f) only depends on the intensive variable (C or S). ψ is the sum of two terms: a configurational entropy term, identical to the entropy in f [Eq. (1)] and another term which combines energetics (T_c/T) and kinetics (Γ_c/Γ_t). This latter term is by no means an internal energy term.

The most stable steady-state configuration corresponds

to the absolute maximum of $\psi(S)$ [Eq. (24)]. Respective stabilities of possible steady states may be assessed from the respective heights of the corresponding maxima of ψ. The technique has been already used to explain stability inversion of two structures of Ni_4Mo under electron irradiation.[11(b)]

Figure 5(a) gives an example of such a ψ function obtained by numerical summation. It is found that depending on the temperature, ψ exhibits one or two maxima: the nonequilibrium phase transition is therefore of second- or first-order respectively, in full agreement with the deterministic model. In the case where cascades involve more than one ballistic exchange ($b > 1$) Eq. (17) must be considered rather than Eq. (18) and the above procedure does not lead anymore to an analytical expression of $P(N)$. One implicit equation for $P(N)$ may be found,[12] but it is of poor use for large b values. We now show how a Fokker-Planck equation may be deduced from the full master equation [Eq. (14)] and lead to reliable results.[13]

VI. CASCADE EFFECTS: FOKKER-PLANCK EQUATION DESCRIPTION

In the general master equation (14), notice that b, the maximum value of k, is much smaller than Ω, the maximum value of N. Indeed, in the thermodynamical limit, Ω becomes infinite, while b is fixed by the physics of the excitation (cascade size). As a consequence, all terms in the rhs of Eq. (14), may be Taylor expanded around their value at N. To the second order in $1/\Omega$, and after simple algebra, we get

$$\frac{dP(N,t)}{dt} = -\frac{\partial}{\partial C}\left[P\hat{\mathcal{V}} - \frac{\partial}{\partial C}\mathcal{D}P\right] \tag{25a}$$

or, equivalently,

$$\frac{dP(N,t)}{dt} = -\frac{\partial}{\partial C}\left[P\mathcal{V} - \mathcal{D}\frac{\partial P}{\partial C}\right], \tag{25b}$$

with

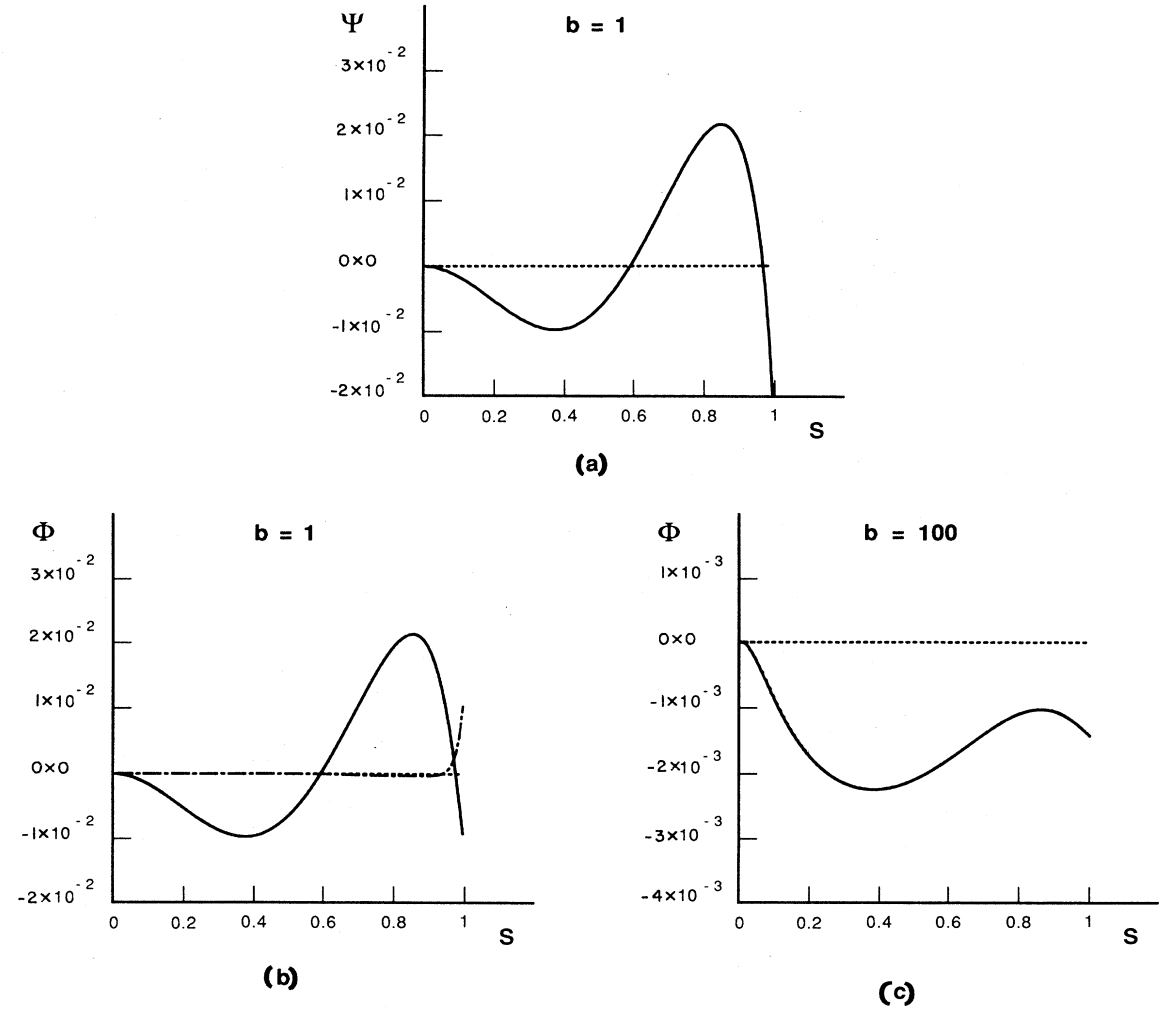

FIG. 5. Stochastic potentials ψ [Eq. (24)] and ϕ [Eq. (30)] for $T/T_c = 0.26$ and $\gamma_0 = 10^{-9}$ with (a) $b = 1$, ψ is obtained directly from the steady-state solution of the master equation; (b) $b = 1$, ϕ is obtained from the Fokker-Planck approximation of the master equation; the (—·—) line represents $\phi - \psi$; (c) $b = 100$, the disordered configuration ($S = 0$) becomes the most stable one. ψ and ϕ are dimensionless.

$$\mathcal{V}=\hat{\mathcal{V}}-\frac{\partial \mathcal{D}}{\partial C} . \tag{25c}$$

In the Fokker-Planck equation (25b) we recognize a diffusion equation where the flux is the sum of a convection ($P\mathcal{V}$) and of a diffusive ($-\mathcal{D}\partial P/\partial C$) contribution. It is found that

$$\hat{\mathcal{V}}(C)=\frac{1}{\Omega}\sum_{k=1}^{b} k\,(W_{N\to N+k}-W_{N\to N-k}) , \tag{26a}$$

$$\mathcal{D}(C)=\frac{1}{2\Omega^2}\sum_{k=1}^{b} k^2(W_{N\to N+k}+W_{N\to N-k}) , \tag{26b}$$

on the rhs of Eqs. (26), for $k>1$, the W's are given by Eq. (16). For $k=1$ the W's are the sum of the ballistic [Eq. (16)] and thermal [Eqs. (15)] contributions. After some algebra we found the following expressions for the ballistic contributions:

$$\hat{\mathcal{V}}^b(C)=\frac{1}{\Omega}b\Gamma_c(1-2C) , \tag{27a}$$

$$\mathcal{D}^b(C)=\frac{1}{2\Omega^2}b\Gamma_c[2C(1-C)+b(1-2C)^2] . \tag{27b}$$

Notice that for a given ballistic jump frequency ($\Gamma_b=b\Gamma_c$), the cascade size appears as a free parameter in the Fokker-Planck equation (FPE) [Eq. (25)] because of the b factor in the diffusion coefficient [rhs of Eq. (27b)]. Therefore, *cascade size effects* are *revealed* by the FPE, while they were not *expected* from the *deterministic description* [Eq. (5)]. We consider now the steady-state solution of the FPE and show first of all that for $b=1$ we recover a solution which is numerically very close to that of the master equation [Eq. (24)] as should be expected;[13] the difference becomes significant only in the near vicinity of $S=1$ [Fig. 5(b)], a value far away from the most stable steady-state value. The latter is not affected. When $b>1$, cascades effects are identified.

The steady-state solution of Eq. (25), provided the systems are conservative, is written as

$$\frac{P(N)}{P(\Omega/2)}=\exp\int_{1/2}^{C}\frac{\mathcal{V}(x)}{\mathcal{D}(x)}dx . \tag{28}$$

Notice that since the W's are all strictly positive quantities, $\mathcal{V}/\mathcal{D}$ is integrable on the interval $[\frac{1}{2},C]$. The argument of the exponential scales with Ω. The extrema of P are given by

$$\mathcal{V}(C)=0 \quad \text{or} \quad \hat{\mathcal{V}}(C)=0 \quad \text{as} \quad \Omega\to\infty . \tag{29}$$

In the thermodynamical limit ($\Omega\to\infty$, C fixed), it is easy to show that the most stable steady-state configuration corresponds to the absolute maximum of $\phi(C)$ given by

$$\phi(C)=\frac{1}{\Omega}\int_{1/2}^{C}\frac{\hat{\mathcal{V}}(x)}{\mathcal{D}(x)}dx . \tag{30}$$

In the particular case where $b=1$, $\phi(S)$ is numerically quite similar to $\psi(S)$ which appears in Eq. (24), as exemplified by Fig. 5(b). Such is no more the case when $b>1$. Figure 5(c) exhibits $\phi(S)$ for $b=100$, but for the same value of γ_0 as in Figs. 5(a) and 5(b). Comparing Figs. 5(b) and 5(c) shows that, whatever the cascade size b, the system exhibits two stable steady-state configurations (maxima of ϕ): one with $S=0$ (disordered state), one with $S\neq 0$ and independent of b. This is to be expected since the extrema of ϕ correspond to $\mathcal{V}=0$ in Eq. (28). As discussed before, $\mathcal{V}$ only depends on the overall ballistic jump frequency $b\Gamma_c$ [Eq. (27a)] and not on b alone. Therefore the possible steady states of the system are not affected by b when γ_0 is kept constant. What is being altered by the cascade size b is the respective stability of the above steady states. Indeed, b appears as a free variable in the noise term $\mathcal{D}$ [Eq. (27b)]. The higher the noise, the shallower the extrema of ϕ. Since $\mathcal{D}$ varies with the degree of order S, the various extrema of ϕ are not affected by the same amount, and stability inversion may be observed on increasing b. Such is the case in Figs. 5(b) and 5(c). In Fig. 5(b), with $b=1$, the disordered state $S=0$ is metastable (local maximum of ϕ) while the ordered one, $S=0.83$, is stable (absolute maximum of ϕ). The reverse is true for $b=100$, γ_0 being kept constant. Notice that, for finite values of Ω, phase coexistence in this context [$\phi_{\max}=\phi(S_1)=\phi(S_2)$] does not imply, because of the preexponential term, equiprobability of the two mesoscopic states S_1 and S_2.[14]

VII. EFFECT OF CASCADES ON THE PHASE DIAGRAM

As previously discussed, cascade effects may inverse the stability of the ordered configuration relative to the disordered one, at a given temperature and overall ballistic jump relative contribution $\gamma=\Gamma_b/\Gamma_t$. Therefore the phase diagram in the γ_0-T/T_c plane is cascade size dependent. However, it is a simple matter to show that the transition line is unaffected as long as it corresponds to a second-order phase transition. Neither the position of the tricritical point nor the spinodal line are affected. Indeed, cascade effects shift the first-order transition line towards the spinodal line. Figure 6 shows the result of a numerical calculation of the transition line, obtained from trial and error computations of ϕ.

Analytically, the spinodal line (which becomes the transition line beyond the tricritical point) is defined by the condition that $\phi(C)$ has an inflexion point for $S=0$, i.e., for $C=\frac{1}{2}$,

$$\left.\frac{\partial^2\phi}{\partial C^2}\right|_{C=1/2}=0 . \tag{31}$$

From Eqs. (30) and (27), simple algebra shows that for $C=\frac{1}{2}$ the coefficient of b which enters $\partial^2\phi/\partial C^2$ because of $\mathcal{D}$ and $\partial\mathcal{D}/\partial C$ vanishes. Therefore the spinodal line is not affected by the cascade size. Similarly, the tricritical point is defined by the condition

$$\left.\frac{\partial^4\phi}{\partial C^4}\right|_{C=1/2}=0 . \tag{32}$$

For the same reasons as above, the latter condition does not depend on b *per se*. Therefore cascade size effects only alter the first-order transition line.

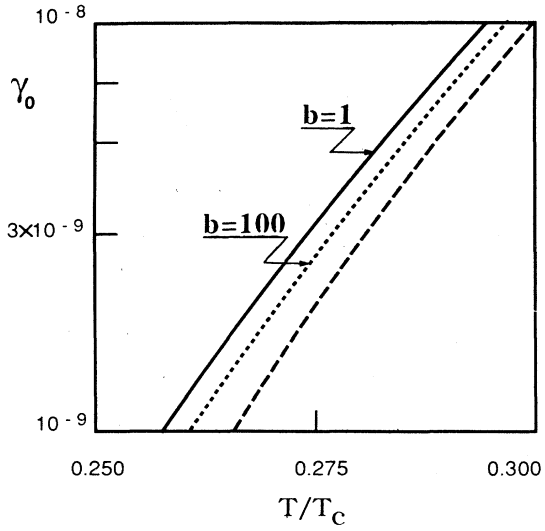

FIG. 6. Cascade size effect on the low-temperature part of the dynamical phase diagram ($T/T_c < 0.422$, $\gamma_0 < \gamma_0^*$). Increasing the cascade size b, at constant γ_0, slightly shifts the first-order transition line towards the spinodal ordering line. γ_0 is dimensionless [Eq. (12a)].

VIII. DISCUSSION AND CONCLUSIONS

Cascade size effects are of practical relevance in metallurgy. They have been qualitatively identified in several cases of irradiation-induced phase transitions. As an example, it is well known that it is "easier" to amorphize a crystalline sample by ion (cascade producing) than by electron (small replacement sequences) irradiation.[15] Similarly, in the first phase diagram under irradiation ever published,[16] one of the coexistence lines was shifted by several hundred degrees when going from e^- to ion irradiation. The above phase transitions are still too complex to be addressed quantitatively by the present model.

However, the present work has derived a technique which should be of more general use than the very simple phase transition just studied. Work is in progress for more complex order-disorder transitions, with several competing structures. Taking spatial heterogeneities into account is the next challenge.

For the time being, we have shown, in the prototype $B2$ order-disorder transition, the following points. When ballistic atomic jumps act in parallel with thermally activated jumps, (i) the phase diagram exhibits a tricritical point at about 0.42 the classical critical temperature; (ii) cascade size is of no influence on the steady state values of the order parameter. The respective stability of the various steady states, however, is altered by the former.

Before the tricritical point ($T < 0.42 T_c$), the phase boundary line in the $\gamma_0 - T$ phase diagram is sensitive to cascade size effects. For a given value of the frequency factor of the ballistic to thermal jump frequency ratio, the larger the cascade size the higher the transition temperature. The phase boundary line is shifted towards the spinodal line.

From the experimental view point, going from light-particle to heavy-particle irradiation at constant flux will mainly affect the displacement to replacement frequency ratio[7] and as a consequence γ_0. The shift of the first-order transition line will appear as small correction, at least for the parameters values used in this study.

ACKNOWLEDGMENT

Useful discussions with Professor J. L. Lebowitz and Dr. P. Cenedese are gratefully acknowledged.

*Present address: CENS-SRMP 91191 Gif sur Yvette CEDEX, France.

[1]H. Haken, *Advanced Synergetics* (Springer, Berlin, 1983).

[2](a) F. Schlögl, Phys. Rep. **62**, 267 (1980); (b) H. K. Janssen, Z. Phys. **270**, 67 (1974).

[3]R. Landauer, J. Appl. Phys. **33**, 2209 (1962).

[4]For a recent workshop, see *Non Linear Phenomena in Materials Science,* edited by L. Kubin and G. Martin (Trans. Tech., Aedermannsdorf, 1988).

[5]G. Martin and P. Bellon, Mater. Sci. Forum **15-18**, 1337 (1987).

[6]G. Martin, Phys. Rev. B **30**, 1424 (1984).

[7](a) E. M. Schulson, J. Nucl. Mater. **83**, 239 (1979); (b) R. S. Averback and D. N. Seidman, Mater. Sci. Forum **15-18**, 963 (1987).

[8](a) P. L. Garrido, A. Labarta, and J. Marro, J. Stat. Phys. **49**, 551 (1987); (b) R. Dickman, Phys. Lett. A **122**, 463 (1987); (c) J. M. Gonzalez-Miranda, P. L. Garrido, J. Marro, and J. L. Lebowitz, Phys. Rev. Lett. **59**, 1934 (1987).

[9]F. C. Nix and W. Schockley, Rev. Mod. Phys. **10**, 1 (1938).

[10](a) G. J. Dienes, Acta Metall. **3**, 549 (1955); (b) G. H. Vineyard, Phys. Rev. **102**, 981 (1956).

[11](a) P. Bellon and G. Martin, in Ref. 4, p. 109; (b) P. Bellon and G. Martin, Phys. Rev. B **38**, 2570 (1988).

[12]R. Görtz and D. F. Walls, Z. Phys. B **25**, 423 (1976).

[13](a) W. Horsthemke and L. Brenig, Z. Phys. B **27**, 341 (1977); (b) W. Horsthemke, M. Malek-Mansour, and L. Brenig, Z. Phys. B **28**, 135 (1977).

[14]G. Nicolis and J. W. Turner, Ann. N. Y. Acad. Sci. **316**, 251 (1979).

[15]For example, see J. L. Brimhall, H. E. Kissinger, and L. A. Charlot, Radiat. Eff. **77**, 273 (1983).

[16]A. Barbu, Commissariat à l'Energie Atomique Report No. R-4936, 1978 (unpublished).